Indoor Positioning System Based on Fusion of UWB and IMU with Strong Tracking Kalman Filter

Tianrui Liao, Kaoru Hirota, Zelong Zhang, Xiangdong Wu, Yaping Dai, Zhiyang Jia [*1]

[*1]School of Automation, Beijing Institute of Technology, Beijing 100081, China
E-mail: tianrui-liao@bit.edu.cn

Abstract. A Loosely-Coupled Fusion Positioning (LCFP) system is designed, which integrates Ultra Wide Band(UWB) and Inertial Measurement Unit(IMU) sensor information to locate, and is conducive to suppress the electromagnetic interference to UWB and the error accumulation of IMU. Traditional fusion positioning framework uses Kalman filter for data fusion, which is difficult to process non-Gaussian observation noise. To improve the problem, this system uses Strong tracking Kalman Filter(SKF) for UWB and IMU data fusion, which is conducive to suppress the influence of non-Gaussian noise and improves the positioning accuracy of the system. In the dynamic positioning experiments with non-Gaussian observation noise, the maximum positioning error of this system is about 2 cm lower than that of the traditional fusion positioning system, and the accuracy is improved by about 14%. This means that data fusion using SKF really helps to suppress the effects of non-Gaussian observation noise on the system and enables the system to achieve higher accuracy. In the future, this system framework will not only be applied to the fusion positioning system of UWB and IMU, but also to other fusion positioning systems susceptible to non-Gaussian observation noise, such as UWB and lidar fusion positioning system.

Keywords: Indoor positioning system; Fusion positioning system; Strong tracking Kalman filter; UWB positioning; IMU positioning

1. INTRODUCTION

For indoor positioning scenes, GPS positioning technology is difficult to receive signal, and it is difficult to apply to short-range navigation[1]. Ultra Wide Band (UWB) positioning system stands out among many navigation technologies, and is widely used in indoor navigation positioning[2]. To suppress the influence of electromagnetic interference and NLOS in UWB positioning, UWB and Inertial Measurement Unit(IMU) sensors are often fused[3]. Kalman filter framework is often used for data fusion in fusion positioning system[4]. However, Kalman filter framework has poor performance in dealing with non-Gaussian observation noise[5].

To suppress the influence of observation noise on the system, a Loosely-Coupled Fusion Positioning (LCFP) system is designed. In this system, The coordinate information calculated by UWB and IMU is fused by Strong tracking Kalman Filter(SKF). The output of the system is the tag coordinates calculated by information fusion and filtering.

Kalman filter is difficult to process non-Gaussian noise, which means that traditional fusion positioning systems using Kalman filter are difficult to process non-Gaussian observation noise. In order to solve this problem, SKF is used to fuse UWB and IMU data. The SKF used in this system is optimized to handle non-Gaussian observed noise, which means that this system will be less affected by non-Gaussian observation noise and have higher accuracy when dealing with non-Gaussian observed noise.

Indoor positioning experiments are carried out to verify the positioning accuracy of the system. The experiment is carried out in an indoor environment of 2m*2m. The ROS platform is used to collect positioning data, and MATLAB is used to process and analyze the data.

The method of UWB coordinate solution is introduced in 2. The design of a LCFP system is proposed in 3. The LCFP system based on SKF is introduced in 4. The accuracy of the positioning system is verified by dynamic positioning experiment in 5.

2. UWB POSITIONING COORDINATE SOLUTION

The first step of the TOF positioning algorithm is using the Two-Way(TW) ranging method to measure the distance between the tag and each anchor. The principle of the TW ranging method is shown in **Fig. 1**[6]. And the process of TW ranging in this system are as follows.

(1) The tag sends a Poll signal to the anchor and starts timing.

(2) The anchor delay D_b after receiving Poll signal, and then sends a response signal back to the tag, and starts timing.

(3) After receiving the response signal, the tag records the elapsed time R_a, and sends the final signal to the anchor after delay D_a.

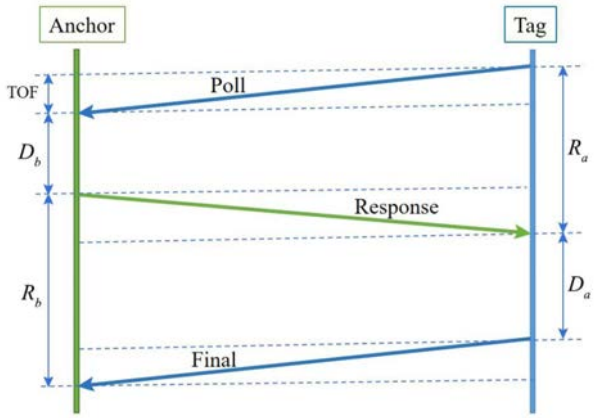

Fig. 1 Schematic diagram of TW ranging method

(4) The anchor stops timing when it receives the final signal, and then records the elapsed time R_b, the flight time t will be calculated as

$$t = \frac{R_a R_b - D_a D_b}{R_a + R_b + D_a + D_b}. \tag{1}$$

(5) It is known that the speed of signal propagation in the air is the speed of light c, so the distance between the anchor and the tag will be calculated.

After calculating the distance from the tag to anchor, the coordinates of the tag will be calculated using the triangulation method, and the schematic diagram is shown in **Fig. 2**[7].

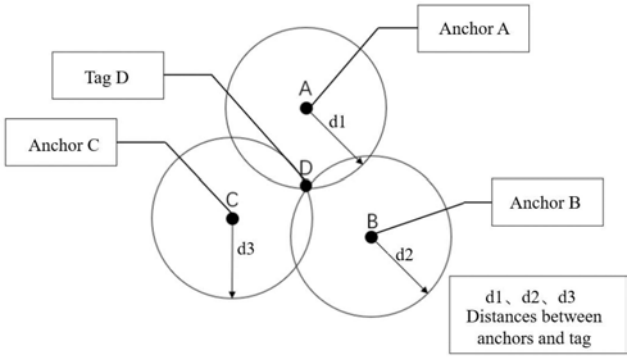

Fig. 2 Schematic diagram of triangulation method

In **Fig. 2**, A, B and C are anchors, D is the requested tag, d_1, d_2, d_3 are the distance between the measured tag and the anchors. The coordinates of the anchors are known, the X_A,X_B,X_C are abscissa, and the Y_A,Y_B,Y_C are ordinates. Then the tag coordinates (X_D, Y_D) will be obtained by

$$\begin{cases} \sqrt{(X_A - X_D)^2 + (Y_A - Y_D)^2} = d_1, \\ \sqrt{(X_B - X_D)^2 + (Y_B - Y_D)^2} = d_2, \\ \sqrt{(X_C - X_D)^2 + (Y_C - Y_D)^2} = d_3. \end{cases} \tag{2}$$

From equation (2), we will get the equation (3).The specific coordinates（X_D, Y_D）of the tag will be obtained by solving equation (3) with less amount of calculation[8].

$$\begin{bmatrix} X_D \\ Y_D \end{bmatrix} = \frac{1}{2}\begin{bmatrix} X_B - X_A & Y_B - Y_A \\ X_C - X_A & Y_C - Y_A \end{bmatrix}^{-1}\begin{bmatrix} r_1^2 - r_2^2 + X_B^2 - X_A^2 + Y_B^2 - Y_A^2 \\ r_1^2 - r_3^2 + X_C^2 - X_A^2 + Y_C^2 - Y_A^2 \end{bmatrix}. \tag{3}$$

In the practical application, electromagnetic interference and NLOS greatly reduce the positioning accuracy of the system[9]. To suppress the influence of these noises, a LCFP system of UWB and Inertial Measurement Unit(IMU) based on Kalman filter is designed.

3. Design of Loosely-Coupled Fusion Positioning System of UWB and IMU Based on Kalman Filter

3.1. Design of positioning system model

For UWB positioning system, it will still be subject to large noise interference after Kalman filtering. The fusion of IMU and UWB will be conducive to solve this problem to a certain extent[10][11]. UWB and IMU are used for LCFP system, and the designed model is shown in **Fig. 3**.

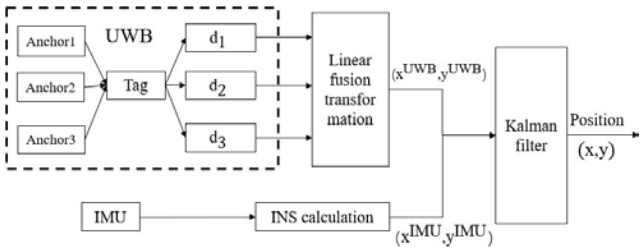

Fig. 3 Model of LCFP system

The system first uses UWB technology to measure the distance between the tag and anchors, and then calculates the tag coordinates（$x_k^{\mathrm{UWB}}, y_k^{\mathrm{UWB}}$）by equation (3). After that, the IMU information is solved to obtain the IMU positioning coordinates ($x_k^{\mathrm{IMU}}, y_k^{\mathrm{IMU}}$). And the Inertial Navigation Solution(INS) process of IMU positioning in this system are as follows [12].

(1) Calculation of velocity and angular velocity.

Because the information measured by IMU sensor only includes acceleration $acc_{x|k}$, $acc_{y|k}$ and angular acceleration $acc_{an|k}$. Therefore, it is necessary to calculate the velocity $v_{x|k}$, $v_{y|k}$ and angular velocity $v_{an|k}$. The calculation process is shown as

$$v_{x|k} = v_{x|k-1} + acc_{x|k-1}T, \tag{4}$$

$$v_{y|k} = v_{y|k-1} + acc_{y|k-1}T, \tag{5}$$

$$v_{an|k} = v_{an|k-1} + acc_{an|k-1}T. \tag{6}$$

(2) Coordinates calculation

Using the velocity and angular velocity information, the angle an_k and coordinates $(x_k^{\mathrm{IMU}}, y_k^{\mathrm{IMU}})$ of this moment will be calculated by

$$an_k = an_{k-1} + v_{an|k-1}T, \tag{7}$$

$$x_k^{\mathrm{IMU}} = x_{k-1} + \cos(an_k)\sqrt{(v_{x|k-1}T)^2 + (v_{y|k-1}T)^2}, \tag{8}$$

$$y_k^{\mathrm{IMU}} = y_{k-1} + \sin(an_k)\sqrt{(v_{x|k-1}T)^2 + (v_{y|k-1}T)^2}. \tag{9}$$

The observation variables for Kalman filter are $(x_k^{\mathrm{UWB}}, y_k^{\mathrm{UWB}})$ and $(x_k^{\mathrm{IMU}}, y_k^{\mathrm{IMU}})$. And the state variables for Kalman filter are (x, v_x, y, v_y), which means x-coordinate, x-direction velocity, y-coordinate and y-direction velocity. Then the state equation and observation equation of this system are expressed as

$$\begin{bmatrix} x_k \\ \dot{x}_k \\ y_k \\ \dot{y}_k \end{bmatrix} = \begin{bmatrix} 1 & T & 0 & 0 \\ 0 & 1 & 0 & 0 \\ 0 & 0 & 1 & T \\ 0 & 0 & 0 & 1 \end{bmatrix} \begin{bmatrix} x_{k-1} \\ \dot{x}_{k-1} \\ y_{k-1} \\ \dot{y}_{k-1} \end{bmatrix} + \begin{bmatrix} \mu_x \\ \mu_{\dot{x}} \\ \mu_y \\ \mu_{\dot{y}} \end{bmatrix}, \tag{10}$$

$$\begin{bmatrix} x_k^{\mathrm{UWB}} \\ y_k^{\mathrm{UWB}} \\ x_k^{\mathrm{IMU}} \\ y_k^{\mathrm{IMU}} \end{bmatrix} = \begin{bmatrix} 1 & 0 & 0 & 0 \\ 0 & 0 & 1 & 0 \\ 1 & 0 & 0 & 0 \\ 0 & 0 & 1 & 0 \end{bmatrix} \begin{bmatrix} x_{k-1} \\ \dot{x}_{k-1} \\ y_{k-1} \\ \dot{y}_{k-1} \end{bmatrix} + \begin{bmatrix} \eta_{x|uwb} \\ \eta_{y|uwb} \\ \eta_{x|imu} \\ \eta_{y|imu} \end{bmatrix}. \tag{11}$$

In the equation (10), T is the work cycle of the system, and the frequency of the system is 50Hz, so $T = 0.02s$. The component of the process noise in x-coordinate at this time is μ_x. The component of the process noise in the x-direction velocity is $\mu_{\dot{x}}$. The component of the process noise in y-coordinate is μ_y. The component of the process noise in the y-direction velocity is $\mu_{\dot{y}}$. The above noises are assumed to satisfy the Gaussian distribution.

In the equation (11), $\eta_{x|\mathrm{uwb}}$ represents the x-component of UWB observation noise, $\eta_{y|\mathrm{uwb}}$ represents the y-component of UWB observation noise, $\eta_{x|\mathrm{imu}}$ represents the x-component of IMU observation noise, $\eta_{y|\mathrm{imu}}$ represents the y-component of IMU observation noise[13] .

3.2. Determination of error covariance matrix

Using Kalman filter to fuse UWB and IMU is essentially a weighted sum of the sampling values of UWB and IMU. The weight of each sample value is determined by the covariance matrix Q of the observation noise. The observation noise covariance matrix Q is determined by the actual measured data, and the tag moves along a straight line in a relatively pure experimental environment. The values of each quantity in the matrix Q are determined by measuring the errors of a and B. the calculation formula is expressed as

$$Q = \begin{pmatrix} \frac{\sum_{k=1}^{n} dx_k^{\mathrm{UWB}} dx_k^{\mathrm{UWB}}}{n} & \frac{\sum_{k=1}^{n} dx_k^{\mathrm{UWB}} dy_k^{\mathrm{UWB}}}{n} & 0 & 0 \\ \frac{\sum_{k=1}^{n} dx_k^{\mathrm{UWB}} dy_k^{\mathrm{UWB}}}{n} & \frac{\sum_{k=1}^{n} dy_k^{\mathrm{UWB}} dy_k^{\mathrm{UWB}}}{n} & 0 & 0 \\ 0 & 0 & \frac{\sum_{k=1}^{n} dx_k^{\mathrm{IMU}} dx_k^{\mathrm{IMU}}}{n} & \frac{\sum_{k=1}^{n} dx_k^{\mathrm{IMU}} dy_k^{\mathrm{IMU}}}{n} \\ 0 & 0 & \frac{\sum_{k=1}^{n} dx_k^{\mathrm{IMU}} dy_k^{\mathrm{IMU}}}{n} & \frac{\sum_{k=1}^{n} dy_k^{\mathrm{IMU}} dy_k^{\mathrm{IMU}}}{n} \end{pmatrix}. \tag{12}$$

In equation (12), variable dx_k^{UWB} is the error of UWB sampling value dy_k^{UWB} when sampling at time k. Variable dy_k^{UWB} is the error of UWB sampling value y_k^{UWB} when sampling at time k. Variable dx_k^{IMU} is the error of IMU sampling value x_k^{IMU} when sampling at time k. Variable dy_k^{IMU} is the error of IMU sampling value y_k^{IMU} when sampling at time k.

To measure the values of the above variables, the label is placed at the point (x, y) to make it move along a straight line to the point (x, y), and the sampling values of UWB and IMU are recorded. The results are shown in **Fig. 4.**

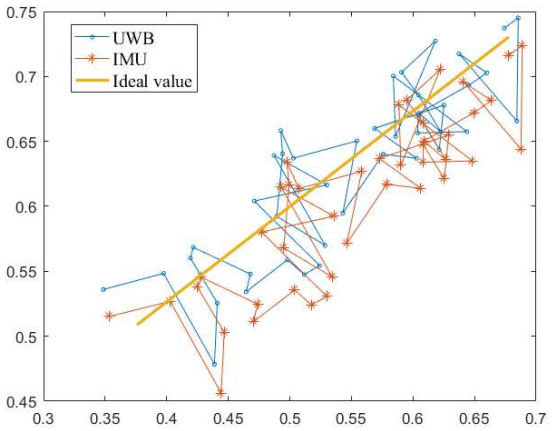

Fig. 4 UWB and IMU sampling values

The values of the covariance matrix of the observation noise error will be calculated from the sampled data, and the results are expressed as

$$\frac{\sum_{k=1}^{n} dx_k^{\mathrm{UWB}} dx_k^{\mathrm{UWB}}}{n} = 0.0014, \tag{13}$$

$$\frac{\sum_{k=1}^{n} dx_k^{\mathrm{UWB}} dy_k^{\mathrm{UWB}}}{n} = 0.0006, \tag{14}$$

$$\frac{\sum_{k=1}^{n} dy_k^{\mathrm{UWB}} dy_k^{\mathrm{UWB}}}{n} = 0.0008, \tag{15}$$

$$\frac{\sum_{k=1}^{n} dx_k^{\mathrm{IMU}} dx_k^{\mathrm{IMU}}}{n} = 0.0016, \tag{16}$$

$$\frac{\sum_{k=1}^{n} dx_k^{IMU} dy_k^{IMU}}{n}=0.0008, \quad (17)$$

$$\frac{\sum_{k=1}^{n} dy_k^{IMU} dy_k^{IMU}}{n}=0.0009. \quad (18)$$

From equations (13) to (18), the value of the error covariance matrix Q will be calculated as

$$Q=\begin{pmatrix} 0.0014 & 0.0006 & 0 & 0 \\ 0.0006 & 0.0008 & 0 & 0 \\ 0 & 0 & 0.0016 & 0.0008 \\ 0 & 0 & 0.0008 & 0.0009 \end{pmatrix}. \quad (19)$$

4. Design of Loosely-Coupled Fusion Positioning System of UWB and IMU Based on Strong Tracking Kalman Filter

Although the LCFP system has high accuracy, the positioning accuracy will still be greatly reduced under the interference of non-Gaussian noise. To suppress the interference of non-Gaussian noise, a LCFP system with SKF is designed, which is conducive to reduce the influence of non-Gaussian noise. The system model is shown in **Fig. 5**.

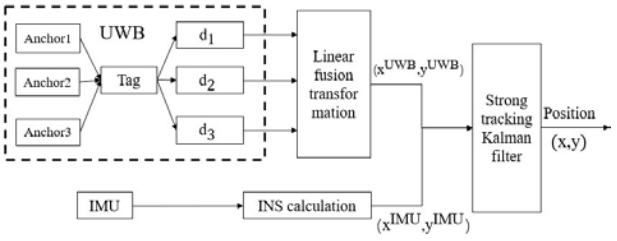

Fig. 5 Model of the LCFP system with SKF

As shown in **Fig. 5**, the system replaces the ordinary Kalman filter with a SKF, which is suitable for processing non-Gaussian observation noise[14]. The SKF is designed as follows.

For SKF, the selected state equation and observation equation are the same as equation (10) and equation (11). And the first two steps of SKF are expressed as

$$\widehat{X}_{k|k-1}=A_{k-1}\widehat{X}_{k-1}+B_{k-1}U_{k-1}, \quad (20)$$

$$P_{k|k-1}=A_{k-1}P_{k-1}A_{k-1}^{T}+Q. \quad (21)$$

After the prediction of state $\hat{x}_{k|k-1}$ and error covariance matrix $P_{k|k-1}$, innovation z_k and innovation covariance C_k will be calculated as

$$z_k=y_k-H_k\widehat{X}_{k|k-1}, \quad (21)$$

$$C_k=\begin{cases} z_k z_k^{T}, k=1, \\ \dfrac{\lambda C_{k-1}+z_k z_k^{T}}{1+\lambda}, k>1, \end{cases} \quad (22)$$

where λ is the forgetting factor and usually $\lambda = 0.95$.

Assuming that the system process noise is constant. When the innovation covariance is large, the conclusion that the observation noise is large will be gotten. At this time, the system needs to expand the initial observation noise covariance matrix R_k. After the innovation covariance C_k is obtained, the proportionality factor β_k is calculated according to the value of C_k, and the noise covariance matrix R_k is expanded as

$$\beta_k=\max(1,\frac{tr(C_k-H_k P_{k|k-1}H_k^{T})}{tr(R_k)}), \quad (23)$$

$$\widetilde{R}_k=\beta_k R_k. \quad (24)$$

Then, according to the expanded observation noise covariance matrix $\tilde{R}_k$, Kalman gain matrix K_k, optimal estimation state $\hat{X}_k$ and error covariance matrix P_k are expressed as

$$K_k=P_{k|k-1}H_k^{T}[H_k P_{k|k-1}H_k^{T}+\widetilde{R}_k]^{-1}, \quad (25)$$

$$\widehat{X}_k=\widehat{X}_{k|k-1}+K_k z_k, \quad (26)$$

$$P_k=[1-K_k H_k]P_{k|k-1}. \quad (27)$$

Through the above steps, the optimal estimation value of tag coordinates （x_k, y_k） will be obtained. This coordinate has higher accuracy in theory, and its specific accuracy needs to be verified by dynamic positioning experiment.

5. Dynamic Positioning Experiments and Result Analysis on LCPF System Based on SKF

The dynamic positioning experiments are used to verify the performance of the system. In the experiments, the ROS platform is used to collect positioning data, and MATLAB is used to process and analyze the data. The experimental environment is shown in **Fig. 6**.

In **Fig. 6**, the coordinates of A0, A1 and A2 of the three anchors are (0,0), (0.83,1.90), (1.66,0). The coordinates of the starting point of the tag trajectory are (0.50,1.20).The tag will pass through the points (0.54,0.36), (0.78,0.40), (0.72, 1.08), (0.99,1.20), and finally will reach the points (1.06,0.40). The trajectory will form an S-shaped path. There is an obstacle under the anchor A1. When the tag is close to the obstacle, the

positioning system will be disturbed by strong non-Gaussian noise.

The reasons for non-Gaussian noise caused by obstacle are as follows[15]. The signal energy of UWB signal will be reduced when it passes through the obstacle, which makes the tag unable to distinguish the direct component from the energy loss of multipath signal. At this time, the system is difficult to detect the direct component. When the system is difficult to detect the direct component, the system may mistakenly regard the multipath component as the direct component. The distance between the tag and the base station calculated by multipath component will increase, resulting in strong non-Gaussian noise.

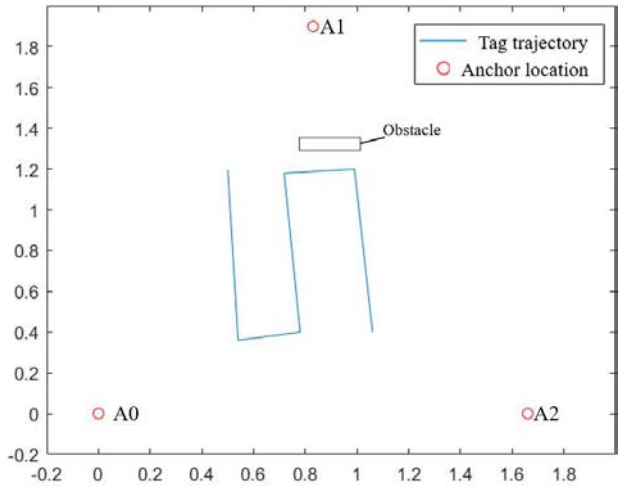

Fig. 6 Schematic diagram of experimental environment

Using the three systems for comparative experiments when the tag moves along the above path. The results are shown in **Fig. 7** and **Fig. 8**. **Fig. 7** shows the comparison of the experimental results between the UWB positioning system and the LCFP system. **Fig. 8** shows the comparison of the experimental results between the LCFP system and the LCFP system based on SKF.

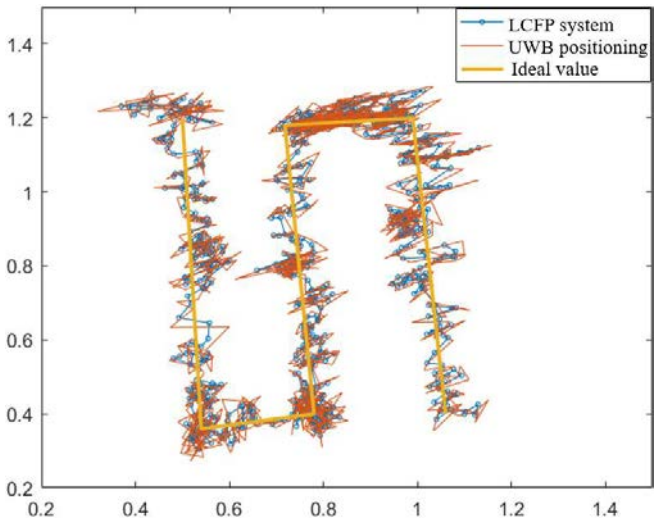

Fig. 7 Experimental results of UWB positioning system and LCFP system

It can be seen from the comparative experimental results that the obstacles in this experiment have a large impact on the positioning accuracy of the system. The closer the tag is to the obstacle, the lower the positioning accuracy of the system. The reason is that when the tag is close to the obstacle, the UWB positioning system is interfered by large non-Gaussian noise, which results in a significant decrease in positioning accuracy.

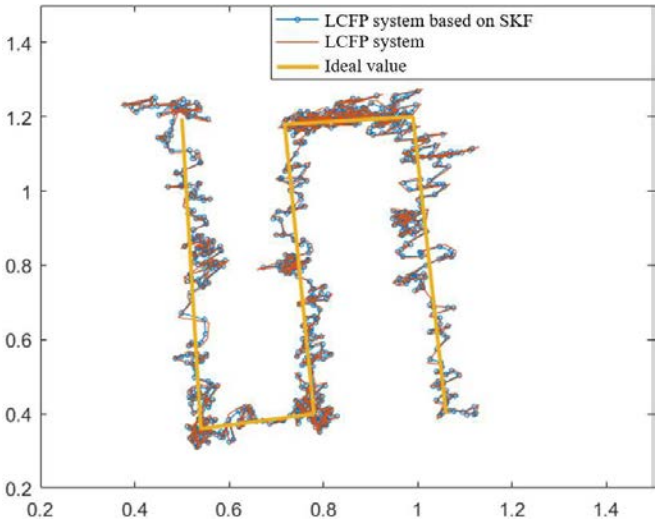

Fig. 8 Experimental results of LCFP and LCFP system based on SKF

Based on the above reasons, the experimental results will be analyzed from three aspects: the whole course positioning results, the positioning results near obstacles and the positioning results away from obstacles. The experimental results are shown in **Table. 1**, **Table. 2** and **Table. 3**.

Table. 1 Experimental results of positioning away from obstacles

Positioning method	*Maximum error*	*Average error*
UWB positioning	0.140m	0.053m
LCFP system	0.095m	0.042m
LCFP system based on SKF	0.091m	0.038m

Table. 2 Experimental results of positioning near obstacles

Positioning method	*Maximum error*	*Average error*
UWB positioning	0.161m	0.092m
LCFP system	0.138m	0.082m
LCFP system based on SKF	0.118m	0.073m

Table. 3 Results of whole course positioning experiment

Positioning method	*Maximum error*	*Average error*
UWB positioning	0.161m	0.061m
LCFP system	0.138m	0.050m
LCFP system based on SKF	0.118m	0.045m

It can be seen from **Table. 1** that when the observation noise of the system meets the Gaussian noise, the LCFP system and the LCFP system based on SKF both play a good filtering effect and improve the positioning

accuracy of the system. And the performance of the two systems is almost the same.

It can be seen from **Table. 2** that when the anchor is blocked, the accuracy of UWB positioning system is greatly reduced due to the interference of non-Gaussian noise. After the information fusion between UWB and IMU, the positioning accuracy of the system is improved by about 11%, which indicates that the LCFP system is conducive to restrain the noise interference of the positioning system to a certain extent. Furthermore, the LCFP system based on SKF has higher accuracy, and its accuracy is improved by about 11% compared with the ordinary LCFP system, which shows that the system has stronger ability to suppress non-Gaussian noise interference.

As can be seen from **Table. 3**, in general, the positioning accuracy of LCFP system based on SKF is the highest one, which is about 26% higher than UWB positioning system and 14% higher than ordinary LCFP system, and is conducive to effectively suppress various noise interference in the positioning process. Experiments show that the LCFP system based on SKF has high positioning accuracy.

The experimental results show that the system is conducive to reduce the influence of non-Gaussian observation noise to some extent when data fusion is performed. Therefore, this system will be suitable for kinds of data fusion systems that may produce non-Gaussian observation noise. In the future, the system framework can be applied to other sensor fusion systems, such as UWB and lidar fusion positioning system, or lidar and photoelectric code disk fusion positioning system, etc.

6. CONCLUSION

The positioning accuracy of the LCFP system based on SKF is verified by dynamic positioning experiment. When the anchor is unblocked, the positioning accuracy of the LCFP system based on SKF is about 35% higher than UWB positioning system but only about 4% higher than ordinary LCFP system.. However, when the anchor is blocked, the positioning accuracy of LCFP system based on SKF is about 26% higher than UWB positioning system and 14% higher than ordinary LCFP system.

The experimental results show that the LCFP system based on SKF does not show obvious advantages when the observation noise basically satisfies the Gaussian distribution. But when the observation noise does not satisfy the Gaussian distribution, the LCFP system based on SKF has better performance than the system using the conventional Kalman filter framework.

Because the system is good at dealing with non-Gaussian observation noise, it can be used in a variety of fusion positioning systems that are susceptible to non-Gaussian observation noise. Such as UWB and lidar fusion positioning system, or lidar and photoelectric code disk fusion positioning system, etc. And the related research has started in laboratory.

Acknowledgements

The authors thanks all those who have contributed to the completion of this article. This work was supported by the Beijing Municipal Natural Science Foundation under Grant No.3192028.

REFERENCES:

[1] P. Shufang, "Research and Development of Positioning System Based on GPS and WIFI," Computer Products and Circulation, No. 9, pp. 115, 2019.

[2] W. Xingxing, and C. Si'an, "A review of indoor positioning research methods," Software Guide, No. 9, pp. 9-12, 2019.

[3] C. Weihan, L, Shiyin. "Indoor precise positioning based on Ultra Wide Band and Micro Inertial Navigation System," Electronic Components and Information Technology, No. 1, pp. 24-26, 2020.

[4] H. Sadruddin, A. Mahmoud and M. Atia, "An Indoor Navigation System using Stereo Vision, IMU and UWB Sensor Fusion," in 2019 IEEE SENSORS, pp. 1-4, 2019.

[5] S. Peng, L. Jizhou, L. pin, Z. Bingqian, and F. Xiangke, "Robust slam method for Inertial / lidar of micro air vehicles in complex environment," Navigation Positioning and Timing, No. 01, pp. 14-21, 2019.

[6] Q. Shi, S. Zhao, X. Cui, M. Lu, and M. Jia, "Anchor Self-Localization Algorithm Based on UWB Ranging and Inertial Measurements," Tsinghua Ence and Technology, No. 06, pp. 728-737, 2019.

[7] F. Dong, C. Shen, J. Zhang and S. Zhou, "A TOF and Kalman filtering joint algorithm for IEEE802.15.4a UWB Locating," in 2016 IEEE Information Technology, Networking, Electronic and Automation Control Conference (ITNEC), 2016, pp. 948-951.

[8] W. Pei, J. Ping, H. Jingjing, and Z. Huimeng, "UWB indoor positioning based on inner triangle centroid algorithm," Computer Applications, No. 01, pp. 289-293, 2017

[9] G. Wei, H. Congyi, X. Wanmin, and C. Xuan, "Research progress and Prospect of indoor navigation and positioning technology," Journal of Navigation and Positioning, No. 01, pp. 10-17, 2019.

[10] Z. Jianming, S. Yuanhao, X. Zhenghe, and W. Jianming, "Adaptive UWB / PDR fusion localization algorithm based on error prediction," Computer Applications, No. 06, pp. 1755-1762, 2020.

[11] H. Benzerrouk and A. V. Nebylov, "Robust IMU/UWB integration for indoor pedestrian navigation," in 2018 25th Saint Petersburg International Conference on Integrated Navigation Systems (ICINS), 2018, pp. 1-5.

[12] Y. Zhipeng, X. Jian, Z. Weisheng, G. hang, and Z. Qilin, "Indoor pedestrian dead reckoning algorithm based on rank Kalman filter," Journal of instrumentation, pp. 01-11, 2020.

[13] T. Xin, W. Guoliang, W. Jianhua, and G. Qi, "Research on improved EKF localization algorithm in NLOS environment," Control Engineering, No. 05, pp. 909-913, 2020.

[14] L. Donghui, W. Jiangqi, X. Kai, H. Bowen, and H. Zhang, "Strong tracking Kalman filter for processing non Gaussian observation noise," Control Theory and Applications, No. 12, pp. 1997-2004, 2019.

[15] Z. Hongmei, Y. Hailong, S. Kunfeng and G. Shuting, "UWB multipath propagation channel characteristics based on time-domain ray tracing," in 2016 2nd IEEE International Conference on Computer and Communications (ICCC), 2016, pp. 1656-1661.